METALURGI
Majalah Ilmu dan Teknologi
p-ISSN 0126-3188 | e-ISSN 2443-3926
ejurnalmaterialmetalurgi.lipi.go.id

THE ADDITION OF C, Zn-C, AND Sn-C ON ANATASE TITANIUM DIOXIDE (TiO_2) FOR DYE-SENSITIZED SOLAR CELLS APPLICATION

Ressa Muhripah Novianti[a], Natalita Maulani Nursam[b,*], Shobih[b], Jojo Hidayat[b], Syoni Soepriyanto[a]

[a]Department of Metallurgical Engineering, Bandung Institute of Technology
Jl. Ganesa No.10, Bandung, Indonesia 40132
[b]Research Center for Electronics, National Research and Innovation Agency
KST Samaun Samadikun, Jl. Sangkuriang-Cisitu, Bandung, Indonesia 40135
*E-mail: natalita.maulani.nursam@brin.go.id

Received: 23-11-2022, Revised: 23-02-2023, Accepted: 28-03-2023

Abstract

DSSC (dye-sensitized solar cell) is a third-generation photovoltaic technology that can convert solar energy into electric current using a photoelectrochemical mechanism. Photoelectrode is one of the significant elements in DSSC, where photoexcited electrons are generated, and serves as an electron transport medium. Anatase titanium dioxide (TiO_2) is often used as photoelectrode material because of its excellent photoactivity, high stability, non-toxicity, environmental friendliness, and low price. Many DSSC modifications have been conducted to overcome the efficiency limitations in DSSC, and one of them is carried out by modifying the TiO_2 via doping. In this study, TiO_2 doped with C and co-doping with Zn (Zn-C) and Sn (Sn-C) were prepared using sol-gel reactions, and they were subsequently applied and tested as photoelectrode in DSSC. The results showed that undoped and doped TiO_2 had a porous spherical morphology with inhomogeneous particle sizes. The addition of C, Zn-C and Sn-C dopants has reduced in the crystallite size and the band gap energy of TiO_2. The efficiency of DSSC with undoped TiO_2 DSSC was 3.83%, while the best performance was obtained from DSSC C-TiO_2 with an efficiency of 4.20%. In contrast, the DSSC with Zn-C-TiO_2 and Sn-C-TiO_2 co-doping produced unexpectedly lower efficiency of 0.71% and 0.85%, respectively.

Keywords: *DSSC (dye-sensitized solar cell), TiO_2, photoelectrode, dopant, efficiency*

1. INTRODUCTION

The increasing human population increased demand for energy sources [1]. Most energy consumed globally comes from non-renewable sources, which will eventually deplete. In addition, using these energy sources can cause environmental pollution [2]. Therefore, it is necessary to have alternative energy sources that can solve this problem. Solar cell is a semiconductor-based device that can convert sunlight directly into electrical current using photovoltaic principles without producing harmful emissions [3]. DSSC (dye-sensitized solar cell) is an emerging technology based on hybrid organic-inorganic materials. Brian O'Regan and Michael Gratzel first discovered the solar cell in 1991. To name a few, DSSC offers the benefit of low production cost, a simple fabrication process, and abundant and environmentally friendly materials [4]-[5].

Photoelectrode is one of the essential elements that determine the performance of DSSC. The semiconductor layer in the photoelectrode acts as a medium to transfer electrons from the dye molecules to the conductive substrate [6]. Titanium dioxide (TiO_2) semiconductor is mostly used as photoelectrode material in DSSC because of its properties, such as excellent photoactivity, chemical stability, non-toxicity, environmental friendliness, and low price. Among the three TiO_2 phases, TiO_2 with an anatase phase is preferred due to its superior optical and physical properties [2].

During the past years, many efforts have been carried out to boost the power conversion efficiency of DSSC, one of which was done by modifying TiO_2 via doping. The choice of

DOI : 10.55981/metalurgi.2023.686

Metalurgi is Sinta 2 Journal (https://sinta.kemdikbud.go.id/journals/profile/3708) accredited by Ministry of Education, Culture, Research, and Technology, Republic Indonesia

dopants for doping on TiO_2 was considered from several things, including the atomic radius. Zn and Sn atoms with atomic radii of 1.42 Å and 1.40 Å, respectively, are the two potential candidates to be substituted into the TiO_2 crystal lattice, replacing some Ti atoms with atomic radii of 1.47 Å. In addition, Zn and Sn also have good electrical properties, are resistant to corrosion, could increase the photoactivity of TiO_2, and could maintain the stability of the anatase TiO_2 phase structure [7]-[9]. In addition to metal dopants, doping using a non-metallic element, such as C atoms with atomic radii 0.7 Å, is also viable because the atomic radius is not much different from the O atom 0.6 Å, thus making it possible to replace the O atom with C atom. C atom also has high photoactivity, good stability, is easy to obtain, and has been reported to help reduce the rate of electron-hole pair recombination [10]-[11].

The doping of TiO_2 could be carried out using various methods, such as hydrothermal, solvothermal, electrospinning, spray pyrolysis, liquid-phase deposition, and the sol-gel method. Among those many methods, the sol-gel method is preferred by many researchers due to its simplicity, and it can be used to obtain nanoparticles with tuneable particle size and homogeneity [12]. In this contribution, we report using the sol-gel technique to synthesize of TiO_2 doped with C and co-doped with Zn (Zn-C) and Sn (Sn-C). This work aims to analyze the effect of such TiO_2 photoanode modifications on the electrical performance of DSSC.

2. MATERIALS AND METHODS

2.1 Materials and Characterizations

The materials used are TTIP (titanium-IV isopropoxide), IPA (isopropyl alcohol), deionized water, aniline, $SnCl_2$ (solid crystalline tin-II chloride), $ZnCl_2$ (zinc chloride), FTO (fluorine-doped tin oxide) substrate, platinum paste, ruthenium dye (Z907), $TiCl_4$ solution, colloidal TiO_2, terpineol, triton, and EL-HPE electrolyte solution.

XRD (x-ray diffraction), SEM-EDX (scanning electron microscope-energy dispersive x-ray spectroscopy), and ultraviolet-visible diffusion reflectance spectroscopy (UV-vis DRS) measurements were conducted to characterize the physical and optical properties of the materials. Meanwhile, current-voltage (I-V) curves and IPCE (incident photon-to-current conversion efficiency) spectra were measured to analyze the resulting DSSC's electrical performance. The I-V characteristics were measured under a solar simulator (Newport) with a light intensity of 500 W/m^2 integrated with an AM1.5G filter.

2.2 Synthesis of Undoped TiO_2 and C-doped TiO_2

The synthesis was initiated by mixing 100 mL of IPA with 10 mL of deionized water and stirring with a magnetic stirrer for 30 min. Then, 1.56 mL of TTIP was added to the solution by dripping slowly using a pipette. For the synthesis of C-doped TiO_2 powder, 100 µL of aniline was added to the solution while stirred for 4 h with a stirring speed of 6000 rpm. As for the synthesis of undoped TiO_2 powder, no aniline was added during the stirring. After stirring, the mixture was allowed to stand at room temperature for 72 hours until a gel precipitate was formed. The gel formed was then separated from the residue. After the gel was separated from the residue, the gel was dried in an oven at 70 °C for 6 h until a solid was formed. The resulting solids of undoped TiO_2 and C-doped TiO_2 were crushed using a mortar until a fine powder was formed. Then, the undoped TiO_2 and C-doped TiO_2 powders were calcined at 450 °C for 3 hours in a vacuum furnace to form the anatase phase.

2.3 Synthesis Zn-C and Sn-C Co-doped TiO_2

Powders of Zn-C and Sn-C co-doped TiO_2 (i.e., with 10 mol % Sn and Zn) were synthesized by dissolving 0.17 g of solid $ZnCl_2$ or 0.24 g of $SnCl_2$ into 50 mL IPA and 10 mL deionized water (solution A). Solution A was stirred for 20 min using a magnetic stirrer. In another glass beaker, 1.56 mL of TTIP was added little by little to 100 mL of IPA and stirred for 30 min using a magnetic stirrer to form a homogeneous solution (solution B). During the stirring of solution B, solution A was slowly poured into solution B, and continued for 4 hours at a stirring speed of 6000 rpm. The following process is the same as the steps in the synthesizing the undoped TiO_2 and C-doped TiO_2 powders.

2.4 Preparation of Undoped TiO_2, C Doped, Zn-C and Sn-C Co-doped TiO_2 Paste

The undoped TiO_2, C-doped, Zn-C, and Sn-C co-doped TiO_2 powder were made into pastes to be attached to the FTO glass by the screen printing method. A colloidal TiO_2 was required to make the paste as a binder to the mixture. The synthesis of colloidal TiO_2 was carried out by mixing 75 mL of deionized water with 2 mL of IPA in a reflux reactor. Then, 12.5 mL of TTIP was added to the mixture by dripping slowly using a pipette while stirring with a magnetic stirrer. After mixing the solution, it was continued by adding 0.6 mL of 65% nitric acid (HNO_3). Next, the reflux reactor was paired with a condenser, heated, and stirred on a hot plate at 80 °C for 8 hours. Upon completion, a white and

slightly transparent colloidal TiO_2 solution was obtained.

To prepare the paste, 0.26 grams of TiO_2/C-TiO_2/Zn-C-TiO_2/Sn-C-TiO_2 powder was crushed with a mortar until a fine powder was produced, and 0.2 mL of colloidal TiO_2 was added and stirred evenly. Then 0.1 mL of terpineol and 0.2 mL of triton were added as a binder solution and stirred evenly until there were no lumps.

2.5 Preparation of Photoelectrodes

Before the coating step, the FTO substrate was coated with a blocking layer by immersing the FTO substrate with 40 mM $TiCl_4$ solution on a hot plate at 70 °C for 30 min. After that, the substrate was rinsed twice using deionized water and dried. The dried substrate was sintered using a muffle furnace at 500 °C for 30 min.

Then the FTO substrate was coated with TiO_2/C-TiO_2/Zn-C-TiO_2/Sn-C-TiO_2 paste using a screen printing method, where the coating was carried out 2 times. The printed FTO substrate will be leveled for 5 min, then dried in the oven at 120 °C for 10 min and sintered in a vacuum furnace at 500 °C for 30 min.

The paste-coated FTO substrate was immersed in $TiCl_4$ solution in the same way as before to produce a TiO_2 reflector layer that increased light absorption in the DSSC.

The following process is the immersion of the samples in Z907 dye solution. The solution was prepared by dissolving 20 mg of Z907 dye powder with 100 mL of ethanol. The immersion was carried out for 24 h at room temperature. After immersion, the substrate was rinsed with ethanol and dried using a hair dryer.

2.6 Preparation of Counter Electrodes

The FTO substrates that have been perforated for electrolyte filling were coated with the platinum paste using the screen printing method. The paste coating process was carried out 2 times and then, the substrate was annealed at 450 °C in a belt conveyor furnace.

2.7 Dye-Sensitized Solar Cell Assembly

The finished photoelectrode and counter electrode were attached with surlyn thermoplastic using a hot press at 125 °C for 40 s. After the two substrates were attached, the EL-HPE electrolyte solution was injected into the gap between the two substrates through the hole on the counter electrode. After the electrolyte solution was filled, the hole on the counter electrode was closed with surlyn thermoplastic and aluminum foil by soldering. The DSSC that had been completely constructed was then coated with conductive silver ink on the sides of the counter electrode and photoelectrode to increase the conductivity during electrical measurements.

3. Result and Discussion

3.1 Crystal Structure

The crystal structure and phase composition of TiO_2, C-TiO_2, Zn-C-TiO_2, and Sn-C-TiO_2 were studied by XRD (x-ray diffraction) analysis, and the results are shown in Fig. 1. It can be seen that the diffraction peaks are relatively sharp, indicating that all samples have good crystallinity. Phase identification was made by matching the measured diffraction peak position data with the JCPDS (joint committee for powder diffraction standard). The diffraction patterns of TiO_2, C-TiO_2, and Zn-C-TiO_2 showed diffraction peaks indicating a single phase, that is, anatase. The typical peak of anatase TiO_2 was found at 2θ (°) 25.3°; 37.8°; and 48.07°, which is the highest intensity peak compared to other anatase diffraction peaks. In Sn-C-TiO_2, apart from the diffraction peak of the anatase phase, one peak indicates the rutile phase at 2θ=27.06°. The anatase phase is typically favourable in DSSC (dye-sensitized solar cell) because it has excellent photoactivity compared to other phases, especially for solar cell applications. This is because the anatase phase has a wider active surface area so that the absorption of dyes will be more optimal and has implications for more photons that can be absorbed [7],[13].

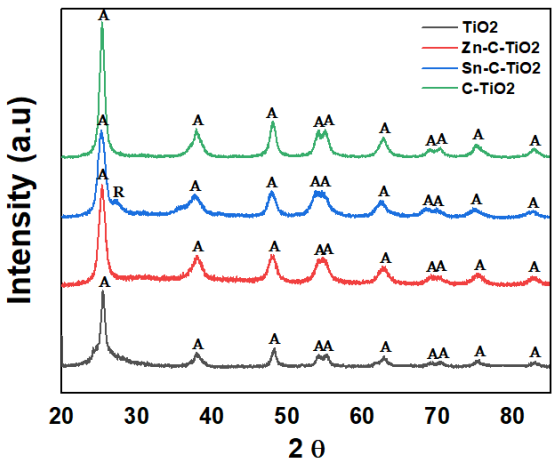

Figure 1. XRD patterns of undoped and various doped TiO_2

The presence of dopant atoms does not change the diffraction pattern. This indicates that the dopant Sn and Zn managed to enter the TiO_2 crystal lattice substituting the Ti atom, while C entered the crystal lattice substituting the O atom. In addition, it is also seen that the presence of dopants indicates an increase in the intensity of the diffraction peak, suggesting enhanced crystallinity. With good crystallinity, the electron injection process in TiO_2 will be faster, and consequently, more photoexcited electrons could

be transferred, which eventually will improve the performance of DSSC [7]-[8],[10],14].

The crystallite size was calcula[ted using the Debye-Scherrer equation as follows:

$$D = \frac{0{,}9\,\lambda}{\beta \cos\theta} \quad (1)$$

where λ is the x-ray wavelength (1.54 Å), β is the FWHM (full widht half maximum), and θ is the diffraction angle (degrees). The calculated crystallite sizes are shown in Table 1.

Table 1. Crystallite size of undoped and doped TiO_2

Samples	Anatase crystallite size (nm)	Rutile crystallite size (nm)	Crystallite size (nm)
TiO_2	87.26	-	87.26
C-TiO_2 1.5	80.49	-	80.49
Zn-C-TiO_2	53.67	-	53.67
Sn-C-TiO_2	56.43	57.65	57.04

The presence of C, Zn-C, and Sn-C dopant led to the formation of TiO_2 with smaller crystal size than that of the undoped TiO_2 due to a decrease in the regularity of the crystal lattice. This is because the presence of C, Zn, and Sn has been reported to slow down the growth of TiO_2 due to differences in atomic radius resulting in several degrees of lattice deformation [15].

3.2 Surface Analysis

The surface morphology of the undoped TiO_2 and doped TiO_2 semiconductors was analyzed using SEM, as shown in Fig. 2. The figure shows that the undoped TiO_2 and C-TiO_2 particles have irregular spherical shapes with inhomogeneous particle sizes. Similar morphology was also observed in Zn-C-TiO_2 and Sn-C-TiO_2, which exhibit inhomogeneous particle shapes and sizes. Many particle aggregates were also present, especially the TiO_2 samples with dopants. The inhomogeneous particle size distribution is likely to be caused by agglomeration. It can be seen that Zn-C-TiO_2 and Sn-C-TiO_2 contain more agglomerations than C-doped TiO_2, so the resulting particles seem relatively larger.

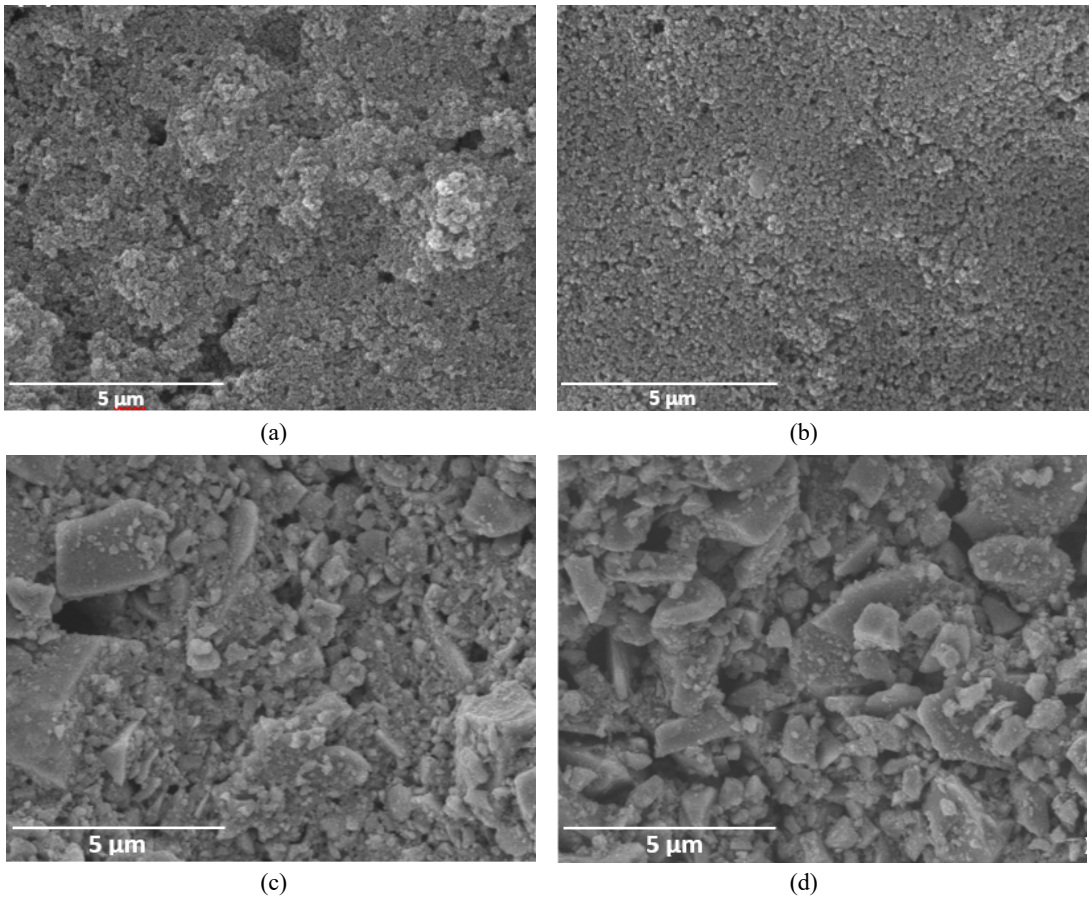

(a) (b) (c) (d)

Figure 2. Surface morphology of (a) TiO_2, (b) C-TiO_2, (c) Sn-C-TiO_2, and (d) Zn-C-TiO_2

In the morphology of the four samples, it can also be seen that some pores could facilitate the dye adsorption into the TiO_2 layer. Consequently, the number of photons that can be absorbed, as well as the redox pairs of the electrolyte, is expected to increase [16]. When more photons are absorbed, more electrons will be injected from the dyes into TiO_2, which will then be transported to the FTO substrate and the outer circuit to produce a higher photogenerated current.

EDX (energy dispersive x-ray spectroscopy) analysis was conducted to determine the elemental composition of undoped TiO_2 and doped TiO_2. The results of EDX are shown in Table 2. The content of elements produced from EDS shows the absence of other unexpected elements. In undoped TiO_2, C content is still obtained, almost the same as C-TiO_2 powder but in different amounts. The C content in undoped TiO_2 is thought to come from the TTIP (titanium-IV isopropoxide) precursor containing carbon and organic chains. Meanwhile, in the C-TiO_2 powder, the C content was attributed to the dopant precursor, aniline, and TTIP. Zn-C-TiO_2 has a minimal Zn element content of 0.59 %wt, while Sn-C-TiO_2 shows a reasonably high Sn element content of 18.16%wt. Dopant content that is too high is typically not expected because it can change the crystal properties of the TiO_2, as seen in the XRD (x-ray diffraction) Sn-C-TiO_2 diffraction pattern with the appearance of the rutile phase.

Table 2. Elemental composition of undoped and doped TiO_2

Sample	Wt (%)				
	Ti	O	C	Zn	Sn
TiO_2	48.46	46.47	5.06	-	-
C-TiO_2	48.44	45.85	5.70	-	-
Zn-C-TiO_2	53.96	41.53	3.92	0.59	-
Sn-C-TiO_2	35.88	41.08	4.88	-	18.16

3.3 UV-Vis DRS Analysis

The values of bandgap energy were calculated using the Kubelka-Munk equation from the measured UV-Vis DRS absorbance data:

$$F(R) = \frac{(1-R)^2}{2R} \quad (1)$$

where R is the reflectance. To estimate the bandgap value, a tangential line was fitted and extrapolated from the Kubelka-Munk absorbance data, and the results are shown in Table 3.

The bandgap energy of synthesized undoped TiO_2 is 3.03 eV, slightly lower than a typical bandgap energy value for anatase TiO_2, which is 3.2 eV. This is likely to be attributed to residual C content in the undoped TiO_2, as previously shown in the EDX results. The presence of this C content will form a new sub-band above the valence band so that it changes the band gap energy value.

The bandgap energy of Zn-C and Sn-C co-doped TiO_2 was 2.92 eV and 2.86 eV, respectively. The presence of Zn-C and Sn-C dopant atoms causes the bandgap energy to decrease due to the synergistic effect of the two dopant types, namely the formation of energy levels above the valence band and below the conduction band, which consequently increases the separation between holes and electrons [17]. These two new sub-bands are very beneficial for photocatalyst applications because the energy required for electron excitation from the valence band to the conduction band is getting smaller to increase the photocatalyst performance. It is different for DSSC applications. The presence of dopants will increase the absorption of the dye on TiO_2 and increase the energy for electron injection from the dye to TiO_2 [6]. This will have implications for the speed of electron transport from TiO_2 to the FTO substrate, followed by the flow of electrons to the external circuit for the current generation.

Table 3. Bandgap energy of undoped TiO_2 and doped TiO_2

Sample	Bandgap Energy (eV)
TiO_2	3.03
C-TiO_2	2.91
Zn-C-TiO_2	2.92
Sn-C-TiO_2	2.86

3.4 Photovoltaic Performance of DSSCs

To determine the performance of the DSSCs, an current-voltage (I-V) characterization test was carried out to obtain several important electrical parameters in the solar cell. These parameters are J_{SC} (short circuit current), V_{OC} (open circuit voltage), FF (fill factor), and power conversion efficiency (η), all of which are summarized in Table 4. The measurements were carried out under standardized solar cell characterization conditions, with irradiation from a solar simulator with an AM1.5G spectrum filter at room temperature.

The photocurrent density – voltage ($J - V$) curves measured on the fabricated DSSCs with various TiO_2 modifications are illustrated in Fig. 3. The value of *Voc, Jsc*, and FF are known to determine the efficiency of DSSC. From the *J-V* curves in Fig. 3 and the electrical parameters in Table 4, the undoped TiO_2 produced DSSC with *Jsc* of 4.24 mA/cm^2, *Voc* of 0.70 V, *FF* of 0.65, and efficiency of 3.83%. From the *J-V* curve, it can be seen that the DSSC with C-doped TiO_2 shows significantly better performance than the DSSC with Zn-C and Sn-C co-doped TiO_2. The DSSC parameters with C-doped TiO_2 produced a *Jsc* of 5.05 mA/cm^2, *Voc* of 0.67 V, *FF* of 0.62, and a power conversion efficiency of 4.21%.

Table 4. Electrical parameters of DSSC with photoelectrode variations

Sampel	Voc (V)	Jsc (mA/cm²)	FF	Efficiency (%)
TiO_2	0.70	4.24	0.65	3.83
C-TiO_2	0.67	5.05	0.62	4.21
Zn-C-TiO_2	0.63	0.92	0.61	0.71
Sn-C-TiO_2	0.68	1.17	0.53	0.85

DSSC with Zn-C and Sn-C co-doped TiO_2 photoelectrodes produced lower DSSC parameters than the C-doped TiO_2 and even the undoped TiO_2. This indicates that the TiO_2 modifications for these two samples did not work as expected. It was observed that during the injection of electrolytes, the electrolyte solutions in Zn-C-TiO_2 and Sn-C-TiO_2 samples were challenging to be infiltrated into the cells.

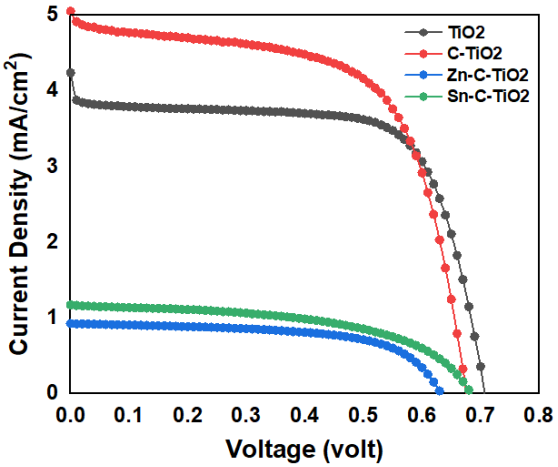

Figure 3. Photocurrent density-voltage curves of DSSCs with TiO_2 photoelectrode variations

The reason was possibly due to the hydrophobicity of the Zn-C-TiO_2 and Sn-C-TiO_2 surface properties [12]. Thus the wetting effect of the photoelectrode by the electrolyte took a lot of work to achieve. In turn, the performance of the DSSC will be affected because this electrolyte solution acts as a charge carrier that collects electrons at the counter electrode and brings electrons back to the dye molecule, resulting in an electron transfer cycle in the cell [19]. When there is insufficient electrolyte solution in the cell, the electron transfer cycle will be disrupted, thereby lowering the current generated by the DSSC.

In addition to the I-V test, IPCE (incident photon-to-current conversion efficiency) testing was also carried out to determine the spectral response of the DSSC. This test was carried out on selected samples that have previously shown high I-V performance for each variation.

Figure 4 shows the IPCE spectra that were collected between 300 to 800 nm. It can be seen that DSSC has a good photoelectric response in the UV light range of 300 – 370 nm and visible light range of 370 – 700 nm. The IPCE curves mainly consist of two absorption regions characterized by the presence of two light absorption peaks, i.e., the first peak was attributed to the light absorption by TiO_2. In contrast, the second peak was attributed to the light absorption by the dye molecules.

In the UV light region, the first peak is formed at a wavelength of 340 nm, which typically corresponds to the absorption band edge of TiO_2. Light absorption by TiO_2 occurs within the short-wave range because TiO_2 has a large band gap energy of around 3.0 – 3.2 eV, so higher energy is required for electron excitation. In the visible light region, the second peak at a wavelength of about 520 nm was mainly attributed to the light absorption by the ruthenium Z907 dyes [20]. The dye absorption that occurs in a longer wavelength range corresponds to the bandgap energy of dye at around ~1.5 eV. Hence the energy required for electron excitation is smaller than that required in TiO_2.

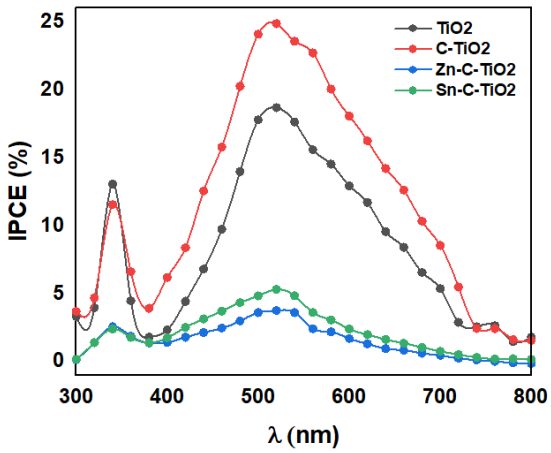

Figure 4. IPCE spectra of DSSCs with TiO_2 photoelectrode variations

The IPCE of DSSC values is determined by the amount of light that the dye can absorb, the number of electrons excited from the dye to the conduction band of TiO_2, and the number of photoexcited electrons transferred from the conduction band of TiO_2 to the external circuit. The highest IPCE value was shown by C-doped TiO_2, indicating that carbon is the most optimal dopant to improve the DSSC performance compared to Zn-C and Sn-C co-doped TiO_2. The higher IPCE value indicates that more photons are converted into the current [20]. The IPCE results align with the results obtained from the current-voltage measurement shown in Fig. 3, where the DSSC with C-doped TiO_2 photoelectrode produced the highest current density.

4. CONCLUSION

TiO_2 photoelectrodes modified with carbon doping and various co-doping were synthesized using a simple sol-gel method, and the resulting materials were applied and tested in DSSC (dye-sensitized solar cell). The presence of C, Zn, and Sn dopants overall decreased bandgap energy and crystal size. DSSC with C-doped TiO_2 achieved the highest performance with a power conversion efficiency of 4.21%. DSSC with co-doping modifications in the form of Zn-C-TiO_2 and Sn-C-TiO_2, produced lower efficiency than the DSSC with pristine TiO_2, which was suspected mainly due to poor wettability at the TiO_2/electrolyte interface.

ACKNOWLEDGMENT

The authors acknowledge support from Advanced PV and Functional Electronic Device research group at the Research Center for Electronics, National Research and Innovation Agency (BRIN) and, the Department of Metallurgical Engineering, Bandung Institute of Technology. E-Layanan Sains (ELSA) BRIN is gratefully acknowledged for access to the materials characterization facilities. This research project was partially funded by Riset dan Inovasi untuk Indonesia Maju or RIIM program by LPDP-BRIN (No. 65/II.7/HK/2022).

REFERENCES

[1] M. S. Ahmad, A. K. Pandey, and N. A. Rahim, "Advancements in the development of TiO_2 photoanodes and its fabrication methods for dye sensitized solar cell (DSSC) applications," *A review Renewable and Sustainable Energy Reviews*, vol. 77, pp. 89-108, 2017. Doi:10.1016/j.rser.2017. 03. 129.

[2] S. Zhuang, M. Lu, N. Zhou, L. Zhou, D. Lin, Z. Peng, and Q. Wu, "Cu modified ZnO nanoflowers as photoanode material for highly efficient dye sensitized solar cells," *Electrochimica Acta*, vol. 294, pp. 28-37, 2019. Doi:10.1016/j.electacta.2018.10.045.

[3] M. Khan, M. R. Al-Mamun, P. K. Halder, and M. A. Aziz, "Performance improvement of modified dye-sensitized solar cells," *Renewable and Sustainable Energy Reviews*, vol. 71, pp. 602-617, 2017. Doi:10.1016/j.rser.2016.12.087.

[4] R. S. Ganesh, K. Silambarasan, E. Durgadevi, M. Navaneethan, S. Ponnusamy, C. Y. Kong, C. Muthamizhchelvan, Y. Shimura, and Y. Hayakawa, "Metal sulfide nanosheet–nitrogen-doped graphene hybrids as low-cost counter electrodes for dye-sensitized solar cells," *Applied Surface Science*, vol. 480, pp. 177-185, 2019. Doi:10.1016/j.apsusc.2019.02.251.

[5] R. S. Ganesh, M. Navaneethan, S. Ponnusamy, C. Muthamizhchelvan, S. Kawasaki, Y. Shimura, and Y. Hayakawa, "Enhanced photon collection of high surface area carbonate-doped mesoporous TiO_2 nanospheres in dye sensitized solar cells," *Materials Research Bulletin*, vol. 101, pp. 353-362, 2018. Doi:10.1016/j.materresbull.2018. 01.018.

[6] L. Zhou, L. Wei, Y. Yang, X. Xia, P. Wang, J. Yu, and T. Luan, "Improved performance of dye sensitized solar cells using Cu-doped TiO_2 as photoanode materials : Band edge movement study by spectroelectrochemistry," *Chemical Physics*, vol. 475, pp. 1-8, 2016. Doi: 10.1016/j.chemphys. 2016.05.018.

[7] B. Li, and N. Tang, "Study on Zr, Sn, Pb, Si and Pt doped TiO_2 photoanode for dye-sensitized solar cells : The first-principles calculations," *Chemical Physics Letters*, vol. 799, pp. 139636, 2022. Doi:10.1016 /j.cplett. 2022.139636.

[8] S. Mehraz, P. Kongsong, A. Taleb, N. Dokhane, and L. Sikong, "Large scale and facile synthesis of Sn doped TiO_2 aggregates using hydrothermal synthesis," *Solar Energy Materials and Solar Cells*, vol. 189, pp. 254-262, 2019. Doi:10.1016/j.solmat.2017. 06.048.

[9] T. C. Paul, J. Podder, and M. H. Babu, "Optical constants and dispersion energy parameters of Zn-doped TiO_2 thin films prepared by spray pyrolysis technique," *Surfaces and Interfaces*, vol. 21, pp. 100725. Doi:10.1016/j.surfin.2020.100725.

[10] N. U. Nor, E. Mazalan, C. Risko, M. Crocker, and N. A. Amin, "Unveiling the structural, electronic, and optical effects of carbon-doping on multi-layer anatase TiO_2 (1 0 1) and the impact on photocatalysis," *Applied Surface Science*, vol. 586, pp. 152641, 2022. Doi:10.1016/j.apsusc.2022.152641.

[11] A. Colombo, C. Dragonetti, D. Roberto, R. Ugo, N. Manfredi, P. Manca, A. Abbotto, G. D. Giustina, and G. Brusatin, "A carbon doped anatase TiO_2 as a promising semiconducting layer in Ru-dyes based dye-sensitized solar cells," *Inorganica Chimica Acta,* vol. 489, pp. 263-268, 2019. Doi: 10.1016/j.ica.2019.02.024.

[12] O. Sadek, S. Touhtouh, M. Rkhis, R. Anoua, M. El Jouad, F. Belhora, and A. Hajjaji, "Synthesis by sol-gel method and characterization of nano-TiO_2 powders,"

Materials Today : Proceedings, 2022. Doi:10.1016/ j.matpr.2022.06.385.
[13] V. R. Gomez, I. M. D. L. Santos, D. S. Jiménez, F. A. Mató, A. Z. Lara, T. R. Bonilla, and M. Courel, "Recent advances in dye sensitized solar cells," *Advances in Materials Science and Engineering,* vol. 836, pp. 1-12, 2019. Doi:10.1007/s00339-019-3116-5.
[14] H. M. Javed, M. Adnan, A. A. Qureshi, S. Javed, M. Adeel, M. Shahid, and M. I. Ahmad, "Morphological, structural, thermal and optical properties of Zn/Mg-doped TiO_2 nanostructures for optoelectronics applications," *Optics & Laser Technology*, 146, pp. 107566, 2022. Doi: 10.1016/j.optlastec.2021.107566.
[15] H. Zhang, Z. Wu, R. Lin, and Y. Wang, "Exploring the mechanism of room temperature ferromagnetism in C-doped TiO_2 nanoclusters by tuning the defects by different annealing temperature using citric acid as C source," *Ceramics International*, vol. 48 (18), pp. 26836-26845, 2022. Doi: 10.1016/j.ceramint. 2022.05.385.
[16] E. M. Bayan, T. G. Lupeiko, L. E. Pustovaya, M. G.Volkova, V. V. Butova, and A. A. Guda, "Zn–F Co-doped TiO_2 nanomaterials: Synthesis, structure and photocatalytic activity," *Journal of Alloys and Compounds*, vol. 822, pp. 153662, 2020. Doi:10.1016/j.jallcom.2020.153662.
[17] S. Mehraz, P. Kongsong, A. Taleb, N. Dokhane, and L. Sikong, "Large scale and facile synthesis of Sn doped TiO_2 aggregates using hydrothermal synthesis," *Solar Energy Materials and Solar Cells*, vol. 189, pp. 254-262, 2020. Doi: 10.1016/j.solmat.2017. 06.048.
[18] S. Aghazada, and M. K. Nazeeruddin, "Ruthenium complexes as sensitizers in dye sensitized solar cells," *Inorganics*, vol. 6, pp. 1-34, 2018. Doi:10.3390/inorganics6020052.
[19] N. Shahzad, Lutfullah, T. Perveen, D. Pugliese, S. Haq, N. Fatima, S. M. Salman, A. Tagliaferro, and M. I. Shahzad, "Counter electrode materials based on carbon nanotubes for dye-sensitized solar cells," *Renewable and Suistanable Energy Reviews*, vol. 159, pp. 112196, 2022. Doi: 10.1016/j.rser.2022.112196.